Cold Regions Science and Technology 92 (2013) 37–47

Contents lists available at SciVerse ScienceDirect

Cold Regions Science and Technology

journal homepage: www.elsevier.com/locate/coldregions

Improved characterisation of sea ice using simultaneous aerial photography and sea ice thickness measurements

Angelika H.H. Renner [a,*], Marie Dumont [a,b], Justin Beckers [c], Sebastian Gerland [a], Christian Haas [c,d]

[a] Norwegian Polar Institute, Fram Centre, Tromsø, Norway
[b] Météo - France - CNRS, CNRM - GAME URA 1357, CEN, Grenoble, France
[c] University of Alberta, Edmonton, Canada
[d] York University, Toronto, Canada

ARTICLE INFO

Article history:
Received 26 September 2012
Accepted 31 March 2013

Keywords:
Sea ice
Photography
Classification
Sea ice thickness
Airborne methods
Arctic

ABSTRACT

We present a semi-automatic classification algorithm for processing of aerial photographs of sea ice in combination with total (sea ice plus snow) sea ice thickness measurements from a helicopter-borne electromagnetic induction device. The algorithm is based on discriminant analysis of spectral and textural features in normalised images using a training set and includes five ice classes. Supervision and optional additional training sets can be used to further reduce misclassifications. The photographs were taken simultaneously with the sea ice thickness measurements and the results from the classification and the thickness data have been merged for more detailed analysis. The algorithm was tested using two case studies from flights over the summer pack ice north of Svalbard and in Fram Strait. The observed ice thickness distribution was very similar in both regions but the results from the classified images revealed considerable differences. The sea ice cover north of Svalbard contained a high fraction of melt ponds and only very little thin or brash ice. In Fram Strait, however, with predominantly advected ice, the ice cover was subject to more ageing and deterioration and included significantly higher fractions of brash ice and submerged ice. The results from the algorithm in combination with the ice thickness provide new information about the state of the observed sea ice and the relationship of present ice types to ice thickness.

1. Introduction

The Arctic sea ice cover has changed drastically over the past 20 years in summer minimum extent (Comiso et al., 2008; Perovich et al., 2012; Stroeve et al., 2008), thickness (e.g. Haas et al., 2008; Kwok et al., 2009), and age (Comiso, 2012; Maslanik et al., 2007). These changes bring along new challenges in the analysis and interpretation of sea ice observations and increase the need for combined datasets measuring different variables simultaneously. While considerable progress has been made in satellite remote sensing of various properties of sea ice, including ice thickness (e.g. Kwok et al., 2009), surface characteristics, etc., thickness remains undersampled. Further, the relationship between thickness and various sea ice parameters such as ice type, surface characteristics, etc. needs further investigation. Currently one of the most successful methods to measure total snow plus sea ice thickness (in the following referred to as ice thickness) on a regional scale is by using an airborne electromagnetic (EM) induction device, a so-called EM-bird (Haas et al., 2009). The EM-bird has been used widely to obtain information about sea ice thickness on a regional scale over large parts of the Arctic (Haas et al., 2008, 2010; Rabenstein et al., 2010; Renner et al., 2013). Peterson et al. (2008) and Prinsenberg et al. (2008) used a similar helicopter-borne EM-system in the Canadian Archipelago. Prinsenberg et al. (2008) also combined EM measurements with aerial photography using video stills, however, the images were not obtained simultaneously with the thickness measurements and were used for visual inspection only and not analysed quantitatively.

The majority of previous studies in the classification of sea ice from remote sensing imagery has focused on detection of melt pond fraction (e.g. Lu et al., 2010; Markus et al., 2003; Rösel and Kaleschke, 2011) and its influence on sea ice albedo (e.g. Pedersen et al., 2009; Perovich et al., 2002). As the Arctic ice cover is moving towards a regime dominated by first-year ice (Maslanik et al., 2011) melt pond formation is enhanced (Ehn et al., 2011) and Rösel and Kaleschke (2012) observed higher than average values for melt pond fraction in summer observed since 2007. Other thin ice types such as nilas or thin grey ice are highly relevant for surface energy fluxes between ocean and atmosphere. Although only very thin and therefore a minor contributor to the total ice volume in the Arctic (see e.g. Kwok et al., 2009, for a breakdown of the major contributors to the Arctic sea ice volume), thin ice forms a lid on the ocean

* Corresponding author. Tel.: +47 77750557.
E-mail address: angelika.renner@npolar.no (A.H.H. Renner).

0165-232X/$ – see front matter © 2013 Elsevier B.V. All rights reserved.
http://dx.doi.org/10.1016/j.coldregions.2013.03.009

obstructing and modifying e.g. energy and gas exchange (e.g. Kaleschke et al., 2004; Loose and Schlosser, 2011; Perovich, 1991). A more dynamic sea ice cover as reported by Hakkinen et al. (2008) is assumed to result in more leads which in turn could enhance nilas and thin ice formation. Due to the dark appearance and the smooth surface, nilas ice is difficult to distinguish from open water in calm conditions in satellite imagery (visible and radar) and photographs. The thickness is at the lower detection limit of 0.1 m for the EM-bird. The combination of images and EM-bird measurements however, could provide more accurate assessments on the presence and thickness of such thin ice.

Several algorithms can be found in the literature to characterise sea ice types from visible and near infrared remote sensing products. The products used in these studies come from either satellite sensors (e.g. Markus et al., 2003; Rösel and Kaleschke, 2011) or aerial photographs and videos (e.g. Inoue et al., 2008; Krumpen et al., 2011; Lu et al., 2008, 2010; Pedersen et al., 2009; Perovich et al., 2002, 2009; Tschudi et al., 2001) and ship-borne videos (Weissling et al., 2009). Many of them are based on the use of manually selected red, green, blue (RGB), or spectral thresholds, and distinguish three main classes: open water, melt ponds, and snow-covered or bare ice (e.g. Inoue et al., 2008; Krumpen et al., 2011; Lu et al., 2010; Perovich et al., 2002). Rösel and Kaleschke (2011) proposed an automatic method based on Principal Component Analysis to retrieve melt ponds from optical satellite remote sensing (Landsat) data based on spectral information. Pedersen et al. (2009) applied a neural network to retrieve the fractions of snow-covered ice, bare ice, brash ice and open water in a continuous series of photographs. They used the overlapping areas of two successive images to standardise the images. The features used for the neural network were chosen according to Fisher Discriminant Analysis and were both textural and spectral. The neural network was very efficient on their continuous series of photographs, but they also found that there was a need for normalisation of the images. Pedersen et al. (2009) compared the results of their classification with EM-bird ice thickness measurements, however, the photographs and the ice thickness data were not obtained during the same flight and therefore did not cover exactly the same ice.

This study aims to provide a new method to combine information on sea ice classes from aerial photographs and simultaneous ice thickness measurements. We developed a method for classification of the aerial images that met several requirements. First, it had to achieve fast processing since the number of images per flight can be in the order of several thousands of images. Second, the method had to work for different light conditions, e.g. partly cloudy or overcast, low sun elevation angle, or clear sky. Finally, it was also supposed to work on several sea ice types characterised by different features, e.g. young ice, first-year ice, or multiyear ice.

In this paper, we first present the experimental set-up for simultaneous measurements of ice thickness and aerial images. Then we describe the method for semi-automatic classification of the images, and the processing of the ice thickness measurements. The third section presents and discusses first results of the combined observations for two flights, one over first-year ice North of Svalbard and one over multiyear ice in Fram Strait. Conclusions are provided in the last section.

2. Data and methods

2.1. Set-up

The Norwegian Polar Institute regularly performs ship-based field campaigns to Fram Strait between Svalbard and Greenland and to the pack ice north of Svalbard. During these campaigns, a helicopter is used to conduct regional surveys of sea ice thickness and other ice properties. An EM-bird (Haas et al., 2009) is towed underneath the helicopter at approximately 15 m height above the sea ice surface measuring the ice thickness. The nominal flying speed of the helicopter is 36 m s^{-1} (70 knots), at a sampling rate of 10 Hz. This results in a point spacing of 3 to 4 m for individual ice thickness measurements. The footprint of the EM-bird is roughly 50 m depending on the exact height of the instrument. The length of the towline for the EM-bird is 20 m, which leads to a helicopter height of approx. 35 m during the flights. In addition to these standard measurements, we also equipped the helicopter with a digital camera (Canon EOS 350D, with a Sigma 17–35 mm lens) to take downward looking images with a sampling frequency of 0.2 Hz. The focal length of the lense was set to 17 mm to cover as wide an area as possible. The resulting footprint of the images taken from the helicopter was about 30×20 m^2. Exposure time and aperture were set to be determined automatically by the camera for each image. Original image size was 3456×2304 pixels. To allow fast processing, the images were resized to 864×576 pixels before classification. The resulting loss of resolution did not affect the results of the classification as the features taken into account here were well defined on scales larger than the area covered by 4×4 pixels in the original image.

2.2. Sea ice classes

In this study, we chose five different classes as indicated in Fig. 1: open water, thin ice, snow-covered or bare thick ice, melt ponds, and submerged ice. We defined submerged ice to be ice that is below the water surface but still visible from above, e.g. at the edge of ice floes. Since the spectral properties of submerged ice and blue melt ponds can be very similar, we also made use of the differences in the surrounding ice classes (presence of open water versus snow-covered or bare ice only) in an optional step in the classification (see Section 3). The thin ice class includes nilas, grey ice and brash ice.

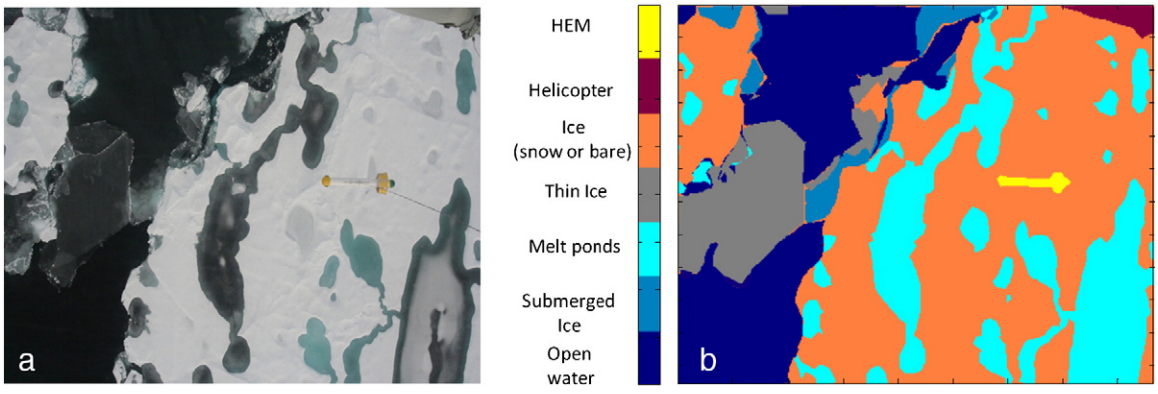

Fig. 1. Aerial photograph (a) and manually classified photograph (b) with the classification chosen in this study. The EM-bird and its towline can be seen in the right part of the image.